Shallow electron centers in silver halides

M. T. Bennebroek, A. Arnold, and O. G. Poluektov
Center for the Study of the Excited States of Molecules, Leiden University, P.O. Box 9504, NL-2300 RA Leiden, The Netherlands

P. G. Baranov
A. F. Ioffe Physico-Technical Institute, Polyteknicheskaya 26, 194021 St. Petersburg, Russia

J. Schmidt
Center for the Study of the Excited State of Molecules, Leiden University, P.O. Box 9504, NL-2300 RA Leiden, The Netherlands
(Received 28 May 1996)

Shallow electron centers in AgCl and AgBr have been studied by pulsed electron nuclear double resonance at 95 GHz. Information about the geometric structure and the ground-state wave function is obtained, which confirms that these centers consist of an electron loosely bound to a Coulombic trap. The microscopic models for these Coulombic traps, to which we are led, differ from the ones suggested from previous optical studies. It appears that the optical transition energies can be reasonably well accounted for by simple hydrogenlike and quantum-defect methods. Owing to the similarity between shallowly trapped and conduction electrons, information about the lowest state of the conduction band is derived, which reveals that this state is not mainly silver *s* like, as is frequently assumed, but also includes a substantial amount of chlorine *s* character. [S0163-1829(96)05039-4]

I. INTRODUCTION

In semiconductors, the incorporation of defects or impurities can strongly influence the electronic properties of the material. Depending on their charge state, such centers can act as Coulombic traps for electrons or holes. When the screening of the Coulombic charge by the lattice is small, the electron or hole will be tightly bound, giving rise to a deep donor or acceptor, respectively. Since for AgCl and AgBr the dielectric constant is relatively large, electrons are loosely bound to centers with an excess positive charge. The resulting shallow donors or shallow electron centers (SEC's) are believed to play an important role in the latent image formation process which occurs in the silver halides when they are irradiated with actinic light.[1,2] The study of SEC's is therefore of technological interest, though, in view of the importance of centers in solids in general, their study is also stimulated by fundamental interest.

Shallow electron centers in silver halides are created upon ultraviolet (uv) excitation, and can be studied at low temperatures. They were first observed in nominally pure crystals by Brandt and Brown using uv-induced infrared-absorption spectroscopy.[3] In a subsequent study, Sakuragi and Kanzaki suggested that SEC's in nominally pure materials are of intrinsic nature, and consist of an electron shallowly trapped at an interstitial Ag^+ ion.[4] When doped with divalent cations like Cd^{2+} or Pb^{2+}, different SEC's appear which, according to these authors, are related to electrons trapped at single Cd^{2+} or Pb^{2+} ions substituting for silver in the lattice. Being paramagnetic, the SEC's can be studied by electron paramagnetic resonance (EPR) experiments.[2] The EPR signals from electrons shallowly trapped by the impurities in AgCl are very similar to those obtained from the intrinsic center and appear as an isotropic, structureless line at $g \sim 1.88$. In AgBr the same features are observed though for the extrinsic SEC's a very small ($\leqslant 0.2\%$) shift from $g \sim 1.49$ of the intrinsic SEC is reported.[2] Since no hyperfine or superhyperfine structure can be resolved, the EPR spectra provide practically no information about the microscopic structure of SEC's.

In a recent paper, we demonstrated that electron nuclear double resonance (ENDOR) spectroscopy at a microwave frequency of 95 GHz can be applied to the study of SEC's in AgCl.[5] The superhyperfine interactions, which are unresolved in EPR experiments, can be detected with this technique, and enable one to derive the position of the center and extent of the delocalization of the shallowly trapped electrons. In the previous paper we focused on the intrinsic SEC in AgCl, and argued that the model proposed by Sakuragi and Kanzaki is incompatible with our results. In this publication we give a more extensive description of the intrinsic SEC in AgCl, include the results obtained for the intrinsic SEC in AgBr, and also those of the Cd- and Pb-related SEC's in AgCl which were used in the previous paper but not published so far. For shallow electrons bound to these closed-shell divalent cations, we are again led to a model different from that proposed by Sakuragi and Kanzaki. A comparison will be made between the experimentally observed transition energies and the values which we calculate using effective-mass theory (EMT) in combination with our ENDOR data. According to EMT the wave function of a shallowly trapped electron resembles that of a conduction electron. The study of SEC's can therefore yield information concerning the nature of the conduction band. It appears that the quantitative results obtained in this study cannot be translated into a simplistic description of the AgCl and AgBr conduction bands.

II. EXPERIMENT

ENDOR studies were performed using a pulsed scheme introduced by Mims.[6] Here a $\pi/2$-τ-$\pi/2$-T-$\pi/2$ microwave

pulse sequence, applied resonantly with the EPR signal of the SEC, produces the so-called stimulated echo (SE) signal at time τ after the third $\pi/2$ pulse. Nuclear transitions are induced by a radio-frequency (rf) pulse, given between the second and third microwave pulses, and monitored as a change of the SE intensity. The ENDOR spectra were recorded via detection of the SE intensity as a function of the radio frequency. For certain frequency regions, nuclear transitions will not affect the SE intensity. These blind spots are a consequence of the pulsed nature of the experiment, and their positions depend on the value of the electron spin S and the value of τ chosen.[6] For a $S=\frac{1}{2}$ system, the blind spots in the $M_S=-\frac{1}{2}$ and $+\frac{1}{2}$ sublevels are located at frequencies $(n/2\tau)$ $(n=0,1,2,...)$ above and below the nuclear Zeeman frequencies. To avoid the possibility of missing individual lines, all ENDOR spectra shown in this paper are constructed from several recordings of small parts (typical widths of 0.5–1 MHz) taken at optimum values of τ.

The experiments were performed on a home-built pulsed EPR and ENDOR spectrometer operating at 95 GHz and 1.2 K, which was described in detail elsewhere.[7] The main advantage of the spectrometer for this work is the high spectral resolution attained in the ENDOR spectra, because the EPR signal of the SEC's appears at a high magnetic field of 3.6 T in AgCl ($g=1.878$) and of 4.6 T in AgBr ($g=1.489$). The rf waves were generated by a computer-controlled Rohde and Schwarz signal generator (model SMS) in combination with either an Electronic Navigation Industries rf power amplifier (model 440 LA) or an Amplifier Research amplifier (model 250L).

Several undoped AgCl crystals were studied as well as a $AgCl:Cd^{2+}$ crystal with an estimated doping level of a few hundred molar parts per million (mppm) and further containing approximately 0.65% of Br^-. Also a ^{111}Cd-enriched AgCl sample was studied with a similar doping level. $AgCl:Pb^{2+}$ and $AgBr:Pb^{2+}$ crystals, with doping levels of about 100 mppm, together with an undoped AgBr crystal, were provided by the Eastman Kodak Company.

In the experiments the sample was cooled from room temperature to 1.2 K without exposure to light. The SEC's were subsequently generated by ultraviolet radiation filtered from a 100-W mercury arc. All experiments were performed under continuous irradiation, because the EPR signal of the SEC's is known to decrease when the light is switched off as a result of recombination of shallowly trapped electrons with hole centers.

III. RESULTS

The ENDOR spectra obtained for the various SEC's in AgCl and AgBr all show a similar pattern. They consist of a multitude of lines symmetrically placed around the nuclear Zeeman frequencies of the silver and halide ions. For the SEC in undoped AgCl the ENDOR spectra of silver, with nuclear transitions of ^{107}Ag($I=\frac{1}{2}$, 52%) and ^{109}Ag($I=\frac{1}{2}$, 48%), and of chlorine, with ^{35}Cl ($I=\frac{3}{2}$, 76%) and ^{37}Cl ($I=\frac{3}{2}$, 24%) transitions, have been shown already in a previous publication.[5] For a quantitative analysis only part of these spectra is needed and in Figs. 1(b) and 2(b) the relevant parts are reproduced for the ^{109}Ag and ^{35}Cl spectra, respectively. These parts contain transitions at frequencies above the nuclear Zeeman frequencies of ^{109}Ag and ^{35}Cl which are revealed by the dips at 7.156 and 15.057 MHz, respectively.

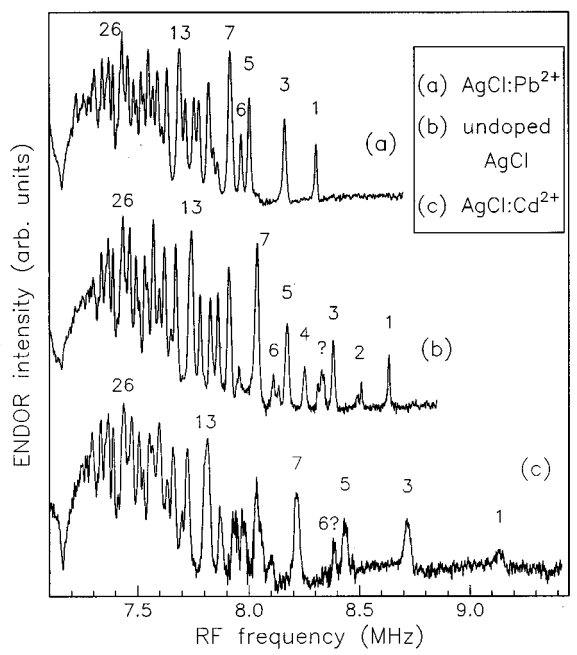

FIG. 1. The high-frequency part of the ^{109}Ag ENDOR spectrum obtained for the shallow electron centers in (a) Pb-doped, (b) undoped, and (c) Cd-doped AgCl crystals. All spectra have been recorded after storage of the samples in the dark at room temperature for a period of months. The ^{109}Ag nuclear Zeeman frequency is positioned at 7.16 MHz. Some of the lines are labeled with shell numbers as discussed in Sec. V.

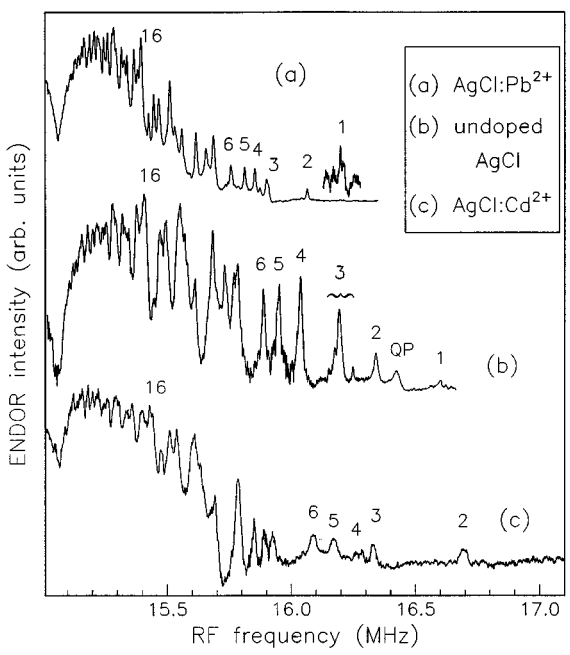

FIG. 2. The high-frequency part of the ^{35}Cl ENDOR spectrum obtained for the shallow electron centers in (a) Pb-doped, (b) undoped, and (c) Cd-doped AgCl crystals. All spectra have been recorded after storage of the samples in the dark at room temperature for a period of months. The nuclear Zeeman frequency of ^{35}Cl is positioned at 15.06 MHz. Some of the lines are labeled with shell numbers as discussed in Sec. V.

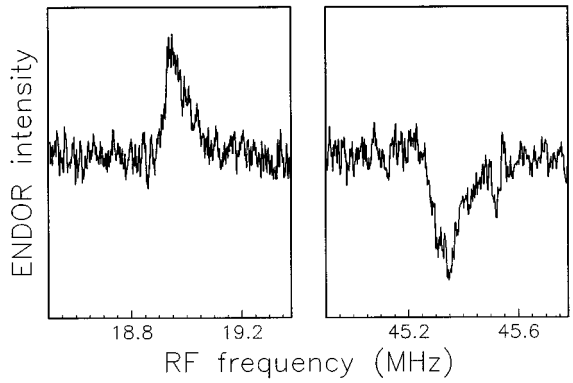

FIG. 3. The ENDOR transitions of ^{207}Pb obtained for the SEC in Pb-doped AgCl. This spectrum has been obtained after storage of the sample in the dark at room temperature for a period of several months.

For comparison we included in these figures the spectra obtained from the Cd^{2+}- and Pb^{2+}-doped AgCl crystals. In the latter crystal it was possible to record nuclear transitions of ^{207}Pb ($I=\frac{1}{2}$, 23%), and the spectrum is shown in Fig. 3. The spectra of the Cd^{2+}- and Pb^{2+}-doped AgCl crystals have been recorded after storage of the doped materials at room temperature in the dark for a long period. If one applies a heat treatment prior to the experiment, the spectra change. This is illustrated in Figs. 4(b) and 4(c), where the ^{109}Ag ENDOR spectra of the Pb^{2+}-doped AgCl crystal are shown after annealing the sample at 350 °C under Ar pressure for a period of 1 and 22 h, respectively, followed by a rapid quench in water. Figure 4(c) resembles the spectrum of the undoped AgCl crystal of Fig. 1(b), whereas Fig. 4(b) is a superposition of this spectrum and the one of the untreated Pb^{2+}-doped AgCl shown in Fig. 1(a) and reproduced in Fig. 4(a). A similar dependence upon heat treatment is observed in the ^{35}Cl ENDOR spectrum.

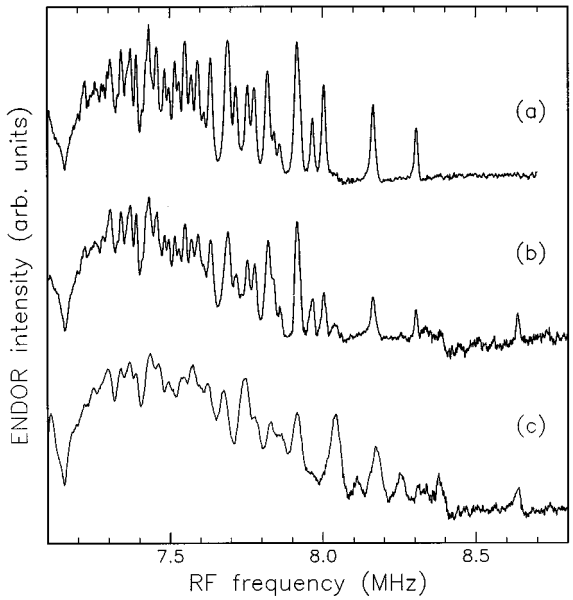

FIG. 4. The dependence of the high-frequency part of the ^{109}Ag ENDOR spectrum of the SEC in AgCl:Pb^{2+} upon heat treatment. (a) was recorded after storage of the crystal at room temperature for a period of several months. (b) and (c) were recorded after annealing the crystal at 350 °C under Ar pressure for periods of 1 and 22 h, respectively, followed by a rapid quench in water.

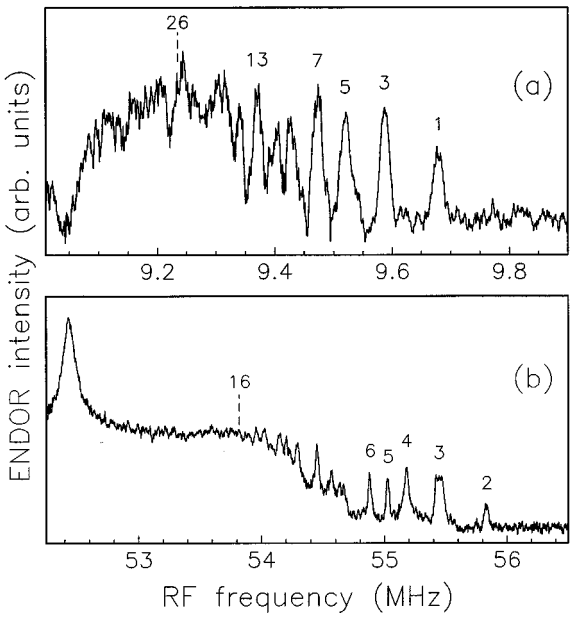

FIG. 5. The high-frequency parts of the ^{109}Ag and ^{81}Br ENDOR spectra of the SEC in undoped AgBr. The corresponding Zeeman frequency is present as a dip in the silver spectrum, but as a peak in the bromine spectrum due to the high rf power that had to be used for the recording of this latter spectrum. Some of the silver and bromine lines are labeled with shell numbers.

The spectra obtained from the SEC in undoped AgBr are depicted in Fig. 5, where part of the ^{109}Ag and ^{81}Br ($I=\frac{3}{2}$, 49%) transitions are shown. The spectral resolution in these spectra is lower compared to that in the spectra of the AgCl crystals, which results from the very low SE signal intensity on which the ENDOR effect is measured. Consequently, high rf powers had to be used to observe any effect at all which in case of the ^{81}Br ENDOR spectrum accounts for the appearance of the Zeeman frequency as a peak instead of a dip.

The silver, chlorine, bromine, and lead ENDOR spectra proved to be isotropic, apart from a few lines in the chlorine and bromine spectra which exhibit a quadrupole splitting. These lines appeared when the magnetic field was oriented along a cubic crystal axis as broad and low intensity lines. When turning the magnetic field away these lines split, become weaker, and broaden even further. Consequently it was not possible to record their orientational dependence.

IV. ANALYSIS

The ENDOR spectra shown in Sec. III can be analyzed using the Hamiltonian

$$H=g_e\beta_e\mathbf{B}_0\cdot\mathbf{s}^e+\sum_{\alpha=1}^{N}\left(-g_{n\alpha}\beta_n\mathbf{B}_0\cdot\mathbf{I}_\alpha+a_\alpha\mathbf{s}^e\cdot\mathbf{I}_\alpha+\mathbf{I}_\alpha\cdot\mathbf{Q}_\alpha\cdot\mathbf{I}_\alpha\right), \quad (1)$$

which describes an electron, with spin operator $\mathbf{s}^e$, coupled to a collection of N nuclei, each with spin operator $\mathbf{I}_\alpha$, in a static magnetic field $\mathbf{B}_0$. The first term on the right describes the isotropic electronic Zeeman interaction with $g_e=1.878\pm0.003$ for AgCl and $g_e=1.489\pm0.004$ for AgBr, whereas the second term accounts for the nuclear Zeeman interactions with $g_{n\alpha}$ the g factor of the nucleus α. Here it is assumed that the nuclear g factor $g_{n\alpha}$ has a positive sign which is the case for most nuclei, like chlorine and bromine. However, for silver nuclei, $g_{n\alpha}$ has a negative sign. The third term describes the isotropic hyperfine (hf) and superhyperfine (shf) interactions with the hyperfine constant a_α given by

$$a_\alpha=\frac{8\pi}{3}\, g_e\beta_e g_{n\alpha}\beta_n|\Psi(\alpha)|^2. \tag{2}$$

Here $|\Psi(\alpha)|^2$ reflects the spin density on nucleus α. From the ENDOR study of the self-trapped exciton in AgCl,[8] it has been established that for silver $a_\alpha<0$ and for chlorine $a_\alpha>0$. This implies, due to the signs of $g_{n\alpha}$, that the density of a shallowly trapped electron is positive on both silver and chlorine nuclei. The traceless tensor $\mathbf{Q}_\alpha$, present in the fourth term of Eq. (1), reflects the quadrupole interaction of the chlorine and bromine nuclei (both $I=\frac{3}{2}$). As mentioned in Sec. III, it was not possible to resolve the orientational dependence of the anisotropic transitions affected by the quadrupole interaction in the AgCl and AgBr crystals. Therefore we will not include the quadrupole interaction in the following analysis.

For an electron ($s^e=\frac{1}{2}$) coupled to a single nucleus α ($I=\frac{1}{2}$ or $\frac{3}{2}$), from Eq. (1), when neglecting the quadrupole term and using first-order perturbation theory, one derives that the ENDOR transitions ($\Delta m_s=0$ and $\Delta M_I=\pm1$) occur at frequencies

$$\nu_{\mathrm{ENDOR}}(\alpha,m_s=\pm\tfrac{1}{2})=\frac{1}{h}\left|g_{n\alpha}\beta_n B_0\mp\frac{a_\alpha}{2}\right|. \tag{3}$$

Thus each nucleus α is expected to give rise to two ENDOR transitions symmetrically placed above and below the nuclear Zeeman frequency $(1/h)g_{n\alpha}\beta_n B_0$. This behavior is indeed observed, as may be verified in the total silver and chlorine ENDOR spectra of the SEC in undoped AgCl published in our previous paper.[5] The fact that a multitude of lines is present in each of the ENDOR spectra indicates that the electron interacts with a large number of lattice nuclei, and therefore is very delocalized. The isotropic behavior of the ENDOR transitions is a manifestation of the diffuse nature of the electron.

According to Eqs. (2) and (3), each line in the ENDOR spectra yields the spin density $|\Psi(\alpha)|^2$ on the nucleus of a particular ion α. In a one-electron model the spin density is directly related to the wave function of the unpaired electron. However in a many-electron system such a simple relationship is lost, and, in order to interpret the spin density, the Schrödinger equation of the entire system, containing not only the unpaired shallow electron but also the core electrons of the lattice ions, should be solved. In ionic crystals this many-electron problem is usually simplified to an effective one-electron problem by the introduction of an envelope function Φ, which refers to the average nature of the wave function of the unpaired electron without consideration of the nodal structure inside the ion cores. Gourary and Adrian argued that, by orthogonalizing a suitable envelope function Φ to the cores of the lattice ions in order to allow for the Pauli principle, the spin density $|\Psi(\alpha)|^2$ on nucleus α may be written as a proportionality constant A_α times the density of the envelope function on that nucleus.[9,10] Thus $|\Psi(\alpha)|^2=A_\alpha|\Phi(\alpha)|^2$. A considerable simplification can be achieved if the envelope function remains approximately constant within each ion core, which seems to be a reasonable assumption for a shallow electron. For this situation, Gourary and Adrian showed that the value of A_α will only depend on the nuclear species of ion α and not on its position in the lattice, i.e., for all silver ions A_α has the same value which is different from the values of A_α for all chlorine or bromine ions. Thus in a one-electron approximation we may rewrite Eq. (2) as

$$a_\alpha=\frac{8\pi}{3}\, g_e\beta_e g_{n\alpha}\beta_n A_\alpha|\Phi(\alpha)|^2. \tag{4}$$

This description is confirmed by effective-mass theory, which specifically applies to a description of shallow donors in solids.[11,12] Here the wave function Ψ of the defect is approximated by

$$\Psi(\mathbf{r})=u(\mathbf{k}_0,\mathbf{r})\cdot F(\mathbf{r}), \tag{5}$$

with $u(\mathbf{k}_0,\mathbf{r})$ representing the lowest Bloch function of the conduction band, and $F(\mathbf{r})$ an envelope function equivalent to the one introduced above. The spin density at nucleus α is then given by $|\Psi(\alpha)|^2=|u(\mathbf{k}_0,\alpha)|^2\cdot|F(\alpha)|^2$, thus again by the density of an envelope function times a proportionality constant. Since Bloch functions possess the periodicity of the lattice, the proportionality constant $|u(\mathbf{k}_0,\alpha)|^2$, by definition, has to be independent of the lattice position of ion α, though its nature still depends on the nuclear species of that ion.

At this point of the analysis we want to derive the spatial distribution of the envelope function Φ from the ENDOR spectrum of a SEC. For this one needs to assign the lines in the ENDOR spectra to the lattice ions, i.e., to determine the position in the lattice of the ion giving rise to a particular ENDOR transition. As a starting point we assumed that the ground state of a SEC resembles a hydrogenlike $1s$ state, thus $\Phi(\mathbf{r})\sim e^{-r/r_0}$. We used a trial-and-error procedure in which $|\Phi(\alpha)|^2$ was calculated on a large number of lattice positions of the cubic silver-halide lattice, trying various center positions of Φ and by optimizing the values of A_{Ag}, A_{Cl}, or A_{Br}, and the Bohr radius r_0, to match the observed shf frequencies.

The results of the analysis of the various SEC's in undoped, Cd^{2+}- and Pb^{2+}-doped AgCl and undoped AgBr are given in Fig. 6, where the density of the envelope function Φ is shown as a function of the radius r. These results were obtained by placing the center of Φ on a Ag^+-lattice position which was the only position, for all SEC's studied by us, that enabled a consistent analysis of both the silver and the halide ENDOR spectra. Accordingly one may define shells consisting of nuclei with the same radius r, and the density of Φ could be derived on a large number of such silver and halide shells; some shells are indicated in the figure. The derived radial defendences for a large part display the expected expo-

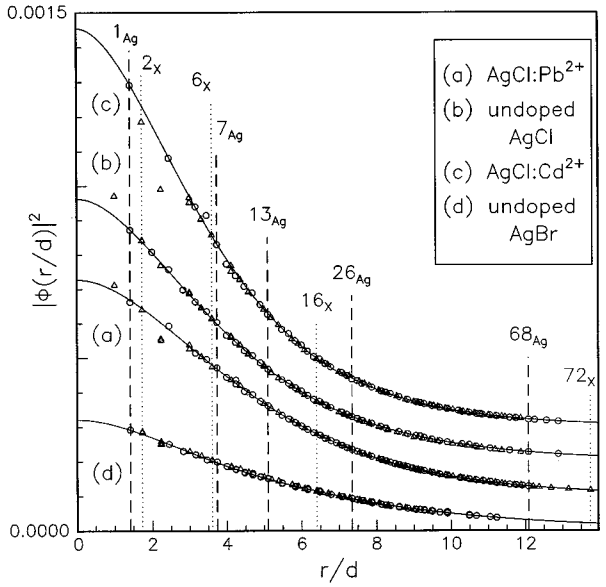

FIG. 6. The density of the envelope function of the various SEC's in AgCl and AgBr as a function of r/d with the interionic lattice distance $d=2.7532$ Å (AgCl) or 2.864 Å (AgBr) at 0 K (Ref. 36). The open circles and triangles denote the densities derived from the silver and halide ENDOR spectra, respectively. The radii of some silver (Ag) and halide (X) shells are indicated. The solid lines represent function (6). The deviation in (b) between this solid line and the derived density of the first chlorine shell at $r=1$ suggests that, for the intrinsic SEC in AgCl, the Cl^- ions directly neighboring the Coulombic trap are displaced. Similarly, the deviations of the first and third (at $r=2.24d$) chlorine shells in case of AgCl:Pb^{2+} [in (a)] and of the third chlorine shell for AgCl:Cd^{2+} [in (c)] suggests a displacement of the involved ions as well.

nential behavior; however, at small radii a distinct deviation is observed. The origin of the deviation from hydrogenic behavior will be discussed in Sec. V.

The radial dependences of Fig. 6 can be approximated by the combined expression

$$|\Phi(\mathbf{r})|^2 \propto \begin{cases} (1+r/r_1)^2 e^{-2r/r_1}, & r \leqslant R_c \\ e^{-2r/r_0}, & r > R_c, \end{cases} \tag{6}$$

where r_0, r_1, and R_c are parameters to be fitted to the experiment. The cuspless part for $r \leqslant R_c$ describes the behavior of Φ close to the binding core, whereas for shells at larger radii the hydrogenlike $1s$ function is more appropriate. Although the combined function (6) does not represent a smooth envelope function at $r=R_c$, it suits our purposes, and we have sketched it in Fig. 6 for the various SEC's. For the SEC in undoped AgCl, we derived $r_0=16.6$ Å, $r_1=9.7$ Å, and $R=16.5$ Å. After normalization of Eq. (6) with these parameters, we obtain a good match of the recorded ENDOR frequencies with $A_{Ag}=3200$ and $A_{Cl}=1370$. The values of A_{Ag} and A_{Cl} or A_{Br} for the other SEC's in AgCl and AgBr are derived in a similar way and collected in Table I.

To check the assignment of the ENDOR lines to the various shells we have made simulations of the recorded ENDOR spectra. This was done by calculating the frequency of an ENDOR transition using Eqs. (6), (4), and (3), and by taking the number of nuclei in a shell as a relative measure for the ENDOR intensity. An example is given in Figs. 7(a) and 7(b), where the simulations of the ^{109}Ag and ^{35}Cl ENDOR spectra of the SEC in Pb^{2+}-doped AgCl are compared with the recorded spectra. These figures show a good overall agreement between the recorded and simulated spectra, especially in the region close to the nuclear Zeeman frequencies, as illustrated in the insets. However, the simulations do not account for all features observed at frequencies above 8 MHz in Fig. 7(a) and above 15.8 MHz in Fig. 7(b). The transitions in these regions originate from nuclei that lie close to the center of Φ, and therefore deviations from the expected ENDOR frequencies carry information about the lattice distortion in the immediate surrounding of the binding core. Simulations of the silver and chlorine ENDOR spectra of the SEC in undoped AgCl were already published in a previous paper,[6] and a comparison with the recorded spectra shows the same features.

TABLE I. The experimentally determined (columns 2, 3, 4, and 5) and theoretically predicted (columns 6 and 7) values of the proportionality constant A_α, which relates the approximate spin density $|\Phi(\alpha)|^2$ to the total spin density $|\Psi(\alpha)|^2$ on a nucleus α. The experimental derivation is discussed in Sec. IV, whereas the theoretical estimates obtained from the point-ion lattice approximation (PILA) and the effective-mass theory (EMT) are described in Sec. V C.

	AgCl			AgBr	Calculated	
	Cd^{2+}	undoped	Pb^{2+}	undoped	PILA	EMT
A_{Ag}	2880	3200	2950	4490	820	1170
A_{Cl}	1260	1370	1270		680	850
A_{Br}				4220	1410	

V. DISCUSSION

In this section we first describe two semiempirical methods for the calculation of the energy levels of the SEC's studied by us. Both are based on envelope functions for the ground states that were derived from ENDOR spectra. Models for the various SEC's will be discussed which are supported by the calculated and experimentally observed values of the energy differences between the ground state and the first few excited states. We end with a more detailed discussion of the wave function of the SEC from which, in principle, information about the electronic structure of the lowest level of the conduction band might be obtained.

A. Description of the energy levels of shallow electron centers

SEC's in silver halides form a typical example of a bound polaron, i.e., a system composed of an electron bound to a Coulombic center and interacting with the lattice polarization field of the ionic crystal. Bound polarons have received wide theoretical interest and are usually classified by two dimensionless parameters.[11] The first is the electron-phonon or Fröhlich coupling constant α, given by $\alpha=\frac{1}{2}[(1/\varepsilon_\infty)-(1/\varepsilon_0)](e^2)/[(\hbar/2m^*\omega_0)^{1/2}](1/\hbar\omega_0)$, which only contains lattice parameters and characterizes the interaction between the bound electron and longitudinal-optical (LO) phonons. For simplicity, all LO modes are represented by the single frequency ω_0; ε_∞ and ε_0 are the high-frequency and the static

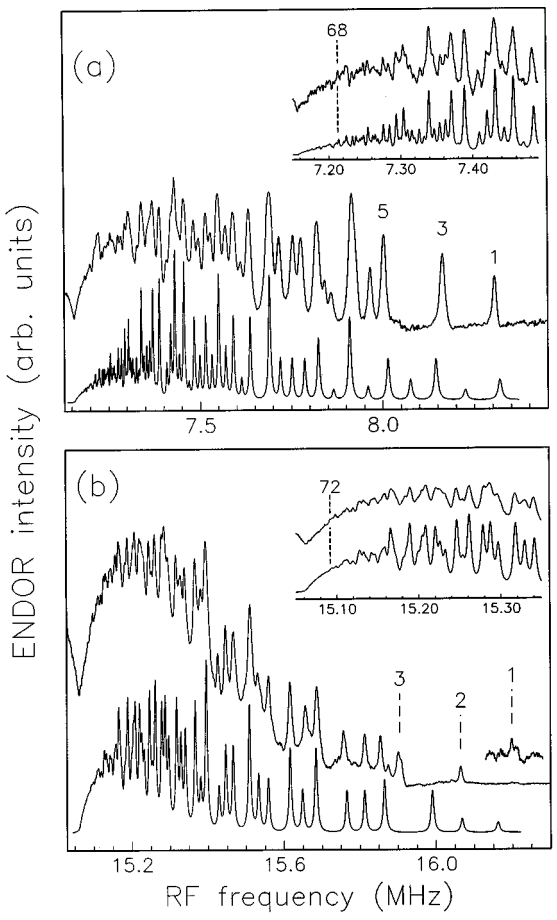

FIG. 7. (a) Comparison between the recorded (upper curve) and simulated (lower curve) high-frequency part of the ^{109}Ag ENDOR spectrum of the SEC in AgCl:Pb^{2+}, obtained after storage of the sample in the dark at room temperature for a period of several months. (b) A similar comparison for the high-frequency part of the ^{35}Cl ENDOR spectrum. The insets illustrate that a good agreement is obtained even in the regions close to the ^{109}Ag and ^{35}Cl nuclear Zeeman frequencies at 7.157 and 15.062 MHz, respectively. The transitions of the 68th silver shell (at 33.3 Å) and of the 72nd chlorine shell (at 37.9 Å) are indicated. We used Lorentzians to represent ENDOR line shapes, and the calculated spectrum is multiplied close to the nuclear Zeeman frequency by the factor $\{1-\cos[2\pi(\nu_{\mathrm{RF}}-\nu_{\mathrm{Zeeman}})2\tau]\}$ to account for the frequency dependence of the ENDOR effect (Ref. 37).

dielectric constants, and m^* the effective band mass for the rigid lattice. The second classification parameter R gives a measure of the Coulombic binding of the electron and is defined as the ratio between the effective Rydberg $R_H^* = (m^*/\varepsilon^2)R_H$ and the LO-phonon energy $\hbar\omega_0$, i.e., $R = (R_H^*/\hbar\omega_0)$.

The present case of SEC's in silver halides belongs to the difficult class of intermediate electron-phonon coupling where $\frac{1}{2}<\alpha<6$ and intermediate binding with $R\approx 1$ (α equals 1.91 and 1.60, and R equals 2.46 and 1.60, for AgCl and AgBr, respectively),[11] which makes a treatment in terms of limiting cases inapplicable. For instance, Matsuura[13] pointed out that the second-order perturbation method, which is considered to be valid in the weak-coupling regime, should not be applied to the intermediate case of the silver halides as was suggested by the approximate results obtained by Bajaj and Clark.[14] According to Stoneham,[11] the present case can be best described by the variational approach of Buimistrov and Pekar. Such a treatment has been applied by Brandt and Brown, who included a model short-range potential to account for the spatial extension of the central Coulombic trap.[3] These authors find a reasonable agreement between the observed and predicted energy levels if the fixed lattice mass is replaced by a slightly reduced mass. However, the validity of this finding is questionable since they used binding energies of 23.8 and 36.2 meV for AgBr and AgCl, respectively, which according to a later publication by Ueta *et al.*[15] should be around 28.5 and 45 meV, respectively. Adamowski applies a method of an optimized canonical transformation which is valid for arbitrary values of the coupling constant α.[16] Since the ionization energies calculated by this method are too large for SEC's in silver halides, it is concluded that the short-range potential neglected in the calculation must be repulsive. Many other treatments exist for the bound polaron problem.[16] In the variational methods, trial functions are introduced to account for the unknown electronic wave functions. Since we are able to derive the ground-state function of a SEC from the ENDOR spectra, we have chosen to use a semiempirical approach for the calculation of its corresponding energy levels.

The simplest description of the energy levels of a shallow electron center resembles that of atomic hydrogen, with an electron of effective mass m^* in a medium of dielectric constant ε. The scaled radius of the lowest $1s$-like energy state is given by

$$r_0=\frac{\varepsilon}{m^*}\,r_H\,, \tag{7}$$

and the binding energy equals

$$E_b=R_H^*=\frac{r_H}{\varepsilon r_0}\,R_H\,. \tag{8}$$

Here r_H is the Bohr radius (0.529 Å), and R_H represents the Rydberg constant (13.6 eV). This so-called effective-mass approximation is appropriate when $r_0 \gg d$, the interionic lattice distance. For AgCl, using the liquid-helium temperature values of the polaron effective mass $m_p=0.431$ (m_0) and the static dielectric constant $\varepsilon_0=9.55$,[17] one expects a radius r_0 of 11.7 Å. Due to the larger static dielectric constant $\varepsilon_0=10.64$ and the smaller polaron mass $m_p=0.2897$ (m_0) in the case of AgBr, shallow electron centers in AgBr should be more delocalized, with r_0 equal to 19.4 Å.

The hydrogenlike $1s$ behavior is reflected in the tail of the radial dependences of the various SEC's shown in Fig. 6. In Table II we have listed the values of r_0 obtained from a fit of these tails to an exponential function. The values of r_0 indicate that SEC's indeed are more delocalized in AgBr than in AgCl, in agreement with the crude estimate given above. With the help of Eq. (8) we can calculate the binding energies E_b based on the values of r_0. When using for ε the value of the static dielectric constant, the values of E_b thus calculated for the SEC's in undoped AgCl and AgBr correspond closely to the values experimentally observed by uv-induced infrared-absorption spectroscopy for the intrinsic SEC's (Ref. 15) (see Table II). Also, the calculated absolute

TABLE II. Comparison of the transition energies of shallow electron centers in AgCl and AgBr obtained from the two semiempirical methods discussed in the text, and from experiment by uv-induced infrared-absorption spectroscopy (Refs. 4 and 15). In the hydrogenlike model (denoted by simple EMT in the table), besides r_0 obtained from the ENDOR data, only the static dielectric constant enters in the calculation. In the quantum-defect method we used δ_{1s}, derived from the ENDOR data, together with $(m^*/\varepsilon^2)(1s)=(m^*/\varepsilon_0^2)=4.726\times10^{-3}$ and $(m^*/\varepsilon^2)(np)=3.175\times10^{-3}$ for AgCl, and $(m^*/\varepsilon^2)(1s)=(m_p^*/\varepsilon_0^2)=2.559\times10^{-3}$ and $(m^*/\varepsilon^2)(np)=2.120\times10^{-3}$ in the case of AgBr.

	Simple EMT				Quantum-defect method				Experimental values (Refs. 4 and 15)		
	r_0 (Å)	E_b (meV)	E_{1s-2p} (meV)	E_{1s-3p} (meV)	δ_{1s}	E_b (meV)	E_{1s-2p} (meV)	E_{1s-3p} (meV)	E_b (meV)	E_{1s-2p} (meV)	E_{1s-3p} (meV)
AgCl:Cd^{2+}	14.7±0.8	51.2±2.8	38.4±2.1	-	−0.125±0.010	50.8±4.8	40.0±3.8	-	-	34.9	-
AgCl:undoped	16.6±0.8	45.4±2.2	34.0±1.6	40.4±1.9	−0.200±0.010	44.7±4.2	33.9±3.2	39.9±3.7	45.0	33.5	40.6
AgCl:Pb^{2+}	18.2±1.1	41.5±2.5	31.1±1.9	-	−0.244±0.010	41.5±3.9	30.7±2.9	-	-	30.5	-
AgBr:undoped	24.8±2.3	27.3±2.5	20.5±1.9	24.3±2.2	−0.124±0.010	27.6±0.8	20.4±0.6	24.4±0.7	28.5	20.8	23.9

energy differences E_{1s-2p} between the hydrogenlike $1s$ and $2p$ states ($E_{1s-2p}=\frac{3}{4}E_b$) and E_{1s-3p} between the hydrogenlike $1s$ and $3p$ states ($E_{1s-3p}=\frac{8}{9}E_b$) match the experimentally observed values, suggesting that SEC's in the undoped materials studied by us are of intrinsic origin. To our knowledge the binding energies E_b of Pb- and Cd-related SEC's have not been reported, but the values of E_{1s-2p} are known.[4] The value of $E_{1s-2p}=30.5$ meV reported for the Pb-related SEC agrees reasonably well with the value 31.1±1.9 meV derived from our ENDOR results for the Pb-doped AgCl crystal. For the Cd-doped AgCl crystal, a significant difference exists between the reported value of $E_{1s-2p}=34.9$ meV and the value 38.4±2.1 meV derived from our experiments. The latter value of E_{1s-2p} is larger than that reported previously[5] because the fit of the radial dependence of the envelope function changed by including additional data points. We will return to this discrepancy below.

Figure 6 illustrates that at small radii the spatial distribution of the various SEC's deviates significantly from the hydrogen $1s$-like behavior. This deviation originates, first of all, from the neglect of the influence of the chemical nature of the Coulombic center in the simple hydrogenlike approximation. This introduces predominantly short-range effects which mostly affect the hydrogen $1s$-like ground state. Second, the interaction of the shallowly trapped electron with the lattice polarization field might also alter the spatial distribution of the electron. According to Stoneham,[11] for the situation of intermediate coupling ($\frac{1}{2}<\alpha<6$) and tight binding ($R\gg1$), a hydrogenlike $1s$ function is best when the electron-phonon coupling is relatively weak ($\alpha^2\ll R$), but as the coupling increases a cuspless form, with a radial dependence described by the first part of Eq. (6), is to be preferred. For the present case of intermediate coupling and binding ($R\approx1$), we find however that the envelope functions of Fig. 6 are best described by a combination of these two functions as expressed by Eq. (6).

The deviation of the density of the envelope functions in Fig. 6 from exponential behavior is only about 5%. Apparently, this deviation is so small that, apart from the Cd-related SEC in AgCl, the simplistic hydrogen model can successfully be applied in the calculation of the energies of the SEC's in AgCl and AgBr. In this model the influence of both the central cell and the electron-phonon interaction is effectively taken into account by the single radius r_0, and it is not possible to determine their separate contributions to the energy levels. Such a separation can be achieved in the quantum-defect method which therefore looks more realistic.

According to the quantum-defect method the energy levels of a shallow donor are given by

$$E_{n,l}=\frac{1}{(n-\delta_{n,l})^2}\frac{m^*}{\varepsilon^2}R_H, \tag{9}$$

and the envelope function of an s-like state can be approximated by

$$\Phi(r)\propto r^{n-\delta_{n,s}-1}\exp\left(-\frac{r}{(n-\delta_{n,s})\frac{\varepsilon}{m^*}r_H}\right). \tag{10}$$

Here the quantum defect $\delta_{n,l}$ accounts for the short-range effect of the Coulombic binding center. From a fit of the radial dependence of the density of the envelope function to Eq. (10) with $n=1$ and using the liquid-helium temperature values of the static dielectric constant ε_0 and the effective polaron mass m_p, we obtain the value of $\delta_{1,s}$. The values for the various SEC's thus derived are listed in Table II and, since they have negative signs, the short-range potential is repulsive in agreement with the prediction made by Adamowski.[16] For SEC's in undoped AgCl and AgBr, we find that the binding energies E_b calculated via Eq. (9) with $n=1$ and $\delta_{1,s}=-0.200\pm0.010$ and $\delta_{1,s}=-0.124\pm0.010$ for AgCl and AgBr, respectively, closely match the experimentally observed values (see Table II). This result seems to justify the use of the polaron mass to account for the electron-phonon interaction in the $1s$-like ground state.

Since the excited np states are very delocalized and have a node at the binding center, their corresponding quantum defect $\delta_{n,p}$ is expected to be negligible. Assuming that the dielectric constant ε and effective mass m^* for the np states have the same values as for the ground state, we can calculate via Eq. (9) the energy differences E_{1s-2p} and E_{1s-3p}. For the SEC in undoped AgCl we obtain $E_{1s-2p}=28.6$ meV and $E_{1s-3p}=37.5$ meV, values which deviate significantly from the experimentally observed energies of 33.5 and 40.6 meV, respectively. A better correspondence is obtained when ε and m^* of the np states are allowed to have different values than in the $1s$ ground state. In principle, when ε and m^* are the same for the $2p$ and $3p$ levels and $\delta_{n,p}\sim0$, one

can derive from Eq. (9) that $(m^*/\varepsilon^2)(np)=\frac{36}{5}\times(E_{1s-3p}-E_{1s-2p})/R_H$. In case of undoped AgCl using the experimental values of E_{1s-2p} and E_{1s-3p}, this leads to $(m^*/\varepsilon^2)(np)=3.758\times10^{-3}$ as compared to $(m^*/\varepsilon^2)(1s)=4.726\times10^{-3}$ for the $1s$-like ground state. Using these ratios we obtain $E_{1s-2p}=31.9$ meV and $E_{1s-3p}=39.0$ meV, which is already closer to the observed values. If one lowers the ratio $(m^*/\varepsilon^2)(np)$ even more to $(m^*/\varepsilon^2)(np)=3.175\times10^{-3}$, the agreement becomes better as can be seen in Table II. With this latter ratio we also find a good agreement between the calculated and observed values of E_{1s-2p} for the SEC in AgCl:Pb^{2+}. In the case of AgCl:Cd^{2+} a significant deviation is found, similar to that given by the simple hydrogen method (see Table II). For the SEC in undoped AgBr, similar features are found. The calculated E_{1s-2p} and E_{1s-3p} values using $(m^*/\varepsilon^2)(np)=(m^*/\varepsilon^2)(1s)=2.559\times10^{-3}$ differ from the experimentally observed values, and a better agreement is obtained if the lower value of 2.120×10^{-3} is used for $(m^*/\varepsilon_2)(np)$.

The results collected in Table II indicate that the ground-state energy of the SEC's in undoped AgCl and AgBr can be calculated reasonably well by the quantum-defect method using the polaron effective mass and the static dielectric constant. The energies of the first excited np states only match the optical data when the effective mass or dielectric constant is modified, which suggests that the electron-phonon coupling is different for these states than for the ground state.

B. Models for the various SEC's

Information about the charge of the cores of the various SEC's is obtained from the results of the ENDOR study of the self-trapped exciton (STE) in AgCl.[8] The STE is formed during ultraviolet excitation, and the ENDOR study confirms that, in its lowest spin-triplet state, it is built up from an electron loosely bound to a self-trapped hole (STH). The electron-spin distribution of the STE can be extracted from the ENDOR data in an identical way as described in Sec. IV and its radial dependence closely resembles that of the SEC's shown in Fig. 6. At large radii the electron behaves like a hydrogenlike $1s$ electron with a Bohr radius $r_0=15.1\pm0.6$ Å. The close agreement of this value with the ones derived for the SEC's in this study, and the fact that the STH is known to have an excess Coulombic charge of $+1$, indicate that the cores of the SEC's have the same Coulombic charge.

1. SEC in undoped AgCl and AgBr

We believe that the shallow electron centers in the undoped AgCl and AgBr crystals studied by us are of an intrinsic nature and not related to impurities, though it is difficult to prove this unequivocally. Support is found in the agreement of the optical transition energies of intrinsic SEC's observed experimentally by Sakuragi and Kanzaki, and the values calculated by us using the two semiempirical methods described above. Common trace impurities like Pb^{2+} $(5d^{10}6s^2)$ and $Cd^{2+}(4d^{10})$ can be excluded, since Figs. 1 and 2 illustrate that electrons shallowly trapped at these divalent cations give rise to different ENDOR spectra. Divalent cations with open valence-shell structures, like Mn^{2+} $(3d^5)$, Fe^{2+} $(3d^6)$ or Cu^{2+} $(3d^9)$, are expected to lead to SEC's with a high-spin $(S>\frac{1}{2})$ ground state, whereas EPR and ENDOR studies confirm that the SEC in undoped silver halides has $S=\frac{1}{2}$. Also, halide contaminants can be ruled out because we find that the SEC must be centered on a Ag^+-lattice position.

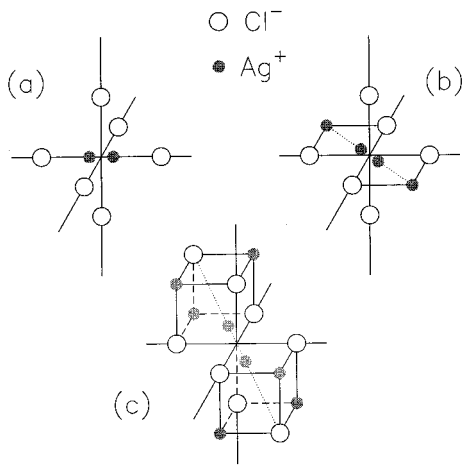

FIG. 8. The three split-interstitial geometries considered for the intrinsic SEC in Sec. V B. Model (a), which possesses D_{4h} symmetry, is not supported by the ENDOR spectra, which point to model (b) with D_{2h} symmetry or geometry (c) with S_6 symmetry. The latter geometry is considered in the Hartree-Fock calculations of Baetzold and Eachus (Ref. 19).

One of the simplest models that can be constructed for an intrinsic SEC consists of an electron loosely bound to a silver ion occupying an interstitial position. However, this model is inconsistent with our result that the intrinsic SEC must be centered on a Ag^+-lattice position. To comply with the latter condition, we suggest the model of a molecular Ag_2^+ ion in which the electron is loosely bound to two adjacent Ag^+ ions in a split-interstitial geometry, i.e., symmetrically placed around a single (vacant) cationic lattice position. Such molecular Ag_2^+ ions have been observed in KCl crystals doped with silver after X irradiation at room temperature.[18] However, in KCl they form deeper electron traps, probably due to the small static dielectric constant of KCl $(\varepsilon_0=4.81)$ as compared to AgCl $(\varepsilon_0=9.55)$ and AgBr $(\varepsilon_0=10.64)$.[17] The model is supported by the results of recent Hartree-Fock calculations by Baetzold and Eachus.[19] They found that the split-interstitial geometry, in which two silver ions lie along a [111] crystal axis with their midpoint on a cationic position [see Fig. 8(c)], forms a plausible structure, and is slightly favored over the normal interstitial position in AgCl at low temperatures. Moreover, this species should act as a shallow electron trap.

The proposed split-interstitial structure should introduce an asymmetric lattice distortion in its direct surrounding, and thereby lead to an asymmetry in the shf interactions with the ions involved. For the intrinsic SEC in AgCl, the silver and chlorine ENDOR spectra clearly indicate the presence of such an asymmetry. As an illustration, we marked with a 2 in Fig. 1(b) the transition that, according to us, originates from the second silver shell. For cubic symmetry, all ions at the six possible [200] positions of this shell would be equivalent, and therefore give rise to a single ENDOR transition. The

TABLE III. The number of equivalent nuclei within the first few silver and chlorine shells surrounding a defect which is centered on a cationic lattice position (taken as [000]). Several local symmetries are considered, of which the latter three correspond to the split-interstitial configurations shown in Fig. 8, and discussed in Sec. V B 1.

Nucleus	Shell number	Shell position	Number of equivalent nuclei O_h	D_{4h}	D_{2h}	S_6
Cl	1	[100]	6	2:4	2:4	6
Ag	1	[110]	12	4:8	2:2:8	6:6
Cl	2	[111]	8	8	4:4	2:6
Ag	2	[200]	6	2:4	2:4	6
Cl	3	[210]	24	8:8:8	4:4:8:8	12:12
Ag	3	[211]	24	8:16	4:4:8:8	6:6:12

observation of two transitions, with a ratio of 1:2, implies that the cubic symmetry is broken. In Table III we list the expected number of equivalent nuclei within each neighboring shell for three possible defect symmetries D_{4h}, D_{2h}, and S_6 which correspond to the three possible orientations of the split-interstitial silver pair shown in Fig. 8. The table illustrates that the 1:2 ratio of the second silver shell is characteristic of a symmetry of D_{4h} or D_{2h}. The splitting of the transitions of the third chlorine shell containing 24 ions at [210] positions and marked with a 3 in Fig. 2(b), indicates that the symmetry is more likely D_{2h}. This suggests that the split interstitial is oriented along a [110] axis [Fig. 8(b)], rather than the [111] orientation considered in the calculations of Baetzold and Eachus, which should reflect S_6 symmetry. No characteristic splitting is observed for the ENDOR transition of the first chlorine shell, marked with a 1 in Fig. 2(b). However, because the calculated shf value for this shell based on an unperturbed lattice is lower than the observed value, which is illustrated in Fig. 6(b) by the deviation of the experimentally derived density at $r=1d$ and the solid line, it seems likely that these Cl^- ions are displaced toward the Coulombic trap. Unfortunately, we cannot find a unique assignment of the lines in both the silver and chlorine ENDOR spectra which allows us to decide between the models shown in Fig. 8. The model of Fig. 8(a) where the split interstitial is oriented along a [100] axis is not supported by the spectra. Moreover, this configuration seems less favorable, as in the other two models of Fig. 8(b) and 8(c) more space is available for the silver pair.

Unfortunately, it is not possible to identify the nuclear transitions of the two central silver ions, forming the split interstitial, in the ENDOR spectrum. In principle, the three possible combinations ^{107}Ag-^{107}Ag, ^{109}Ag-^{109}Ag, and ^{107}Ag-^{109}Ag should give rise to transitions with statistical weights of 23%, 27%, and 50%, respectively. If we assume that the electron density on each of the two central silver ions is half of the density predicted by the radial dependence of Fig. 6(b) for a single ion at $r=0$, we estimate that the transitions of the central silver ions should lie in a region between 7.8 and 8.7 MHz. Such a sharing of electron density has been observed for the molecular Ag_2^+ ion in KCl.[18] In Fig. 1(b) we indicate with a question mark the lines that form possible candidates for the assignment to the central silver pair. In order to test this hypothesis, a ^{109}Ag-enriched AgCl powder was prepared in which the ^{109}Ag-^{109}Ag pair should be dominant. However, this attempt failed because of the bad quality of the powder. Also no information on the central silver ions could be obtained from the ENDOR spectra of the intrinsic SEC in AgBr owing to the low spectral resolution [see Fig. 5(a)].

In principle, information concerning the hf interaction of the central split interstitial might be obtained from the EPR linewidth of the intrinsic SEC's. The full width at half maximum is given by[20]

$$(\Delta B_{1/2})^2=\frac{8\ln 2}{g_e^2\beta_e^2}\sum_{i,l} N_l\xi_i(a_{i,l})^2\cdot\frac{I_{i,l}(I_{i,l}+1)}{3}. \quad (11)$$

Here N_l is the number of nuclei in the lth shell, and ξ_i reflects the relative natural abundance of the isotope. The values of the isotropic shf interaction $a_{i,l}$ for remote shells can be accurately estimated using Eq. (4) with the envelope function (6), in which the parameters have been derived from our analysis, and the values of $a_{i,l}$ for nearby shells are taken directly from the spectra. In this way we estimate $\Delta B_{1/2}=38.2\times10^{-4}$ and 159×10^{-4} T for the intrinsic SEC's in AgCl and AgBr, respectively, which should be compared to the experimental values of $(38.4\pm0.6)\times10^{-4}$ and $(160\pm5)\times10^{-4}$ T. It appears that the EPR linewidth at 1.2 K is completely determined by the shf interaction of the shallowly trapped electron with the lattice ions, and that the contribution of the central pair is negligible. It is to be noted that $\Delta B_{1/2}$ in AgBr is about four times larger than in AgCl as a result of the large gyromagnetic ratio of bromine compared to that of chlorine; as a consequence of the relative small silver gyromagnetic ratio the halide contribution to $\Delta B_{1/2}$ is dominant (81% and 99% in AgCl and AgBr, respectively).

An important question is how intrinsic SEC's are formed at low temperatures. The electron might be trapped on an interstitial silver ion that subsequently is converted to the split-interstitial species. The ENDOR study of the STE in AgCl, however, revealed that an electron with a Bohr radius r_0 of 15.1 Å is too diffuse to alter the geometric structure of its binding core.[8] Therefore one does not expect for intrinsic SEC's that the diffuse electron, with $r_0=16.6$ Å in AgCl and $r_0=24.8$ Å in AgBr, can induce such a conversion, and it seems more likely that the split-interstitial structure already exists before the electron is captured. It can either be ''frozen in'' or created via Frenkel pair formation in the silver sublattice induced by the ultraviolet irradiation. In alkali halides, the formation of Frenkel pairs during ultraviolet irradiation at low temperatures has been observed, but, in contrast to silver halides, this process takes place in the halogen sublattice. It is known that in these materials the Frenkel pairs are created by the nonradiative decay of STE's.[21] A similar process could be active in AgCl, but we doubt its efficiency at low temperatures since no indication of its existence could be found in the ENDOR study of the STE in AgCl.[8] So it seems more likely that the split interstitials are frozen in, which also explains their presence in AgBr where no STE exists. The concentration of intrinsic SEC's is then expected to depend on the experimental and sample conditions which might account for the weakness of the EPR signals we observed for some of the undoped AgCl crystals. For instance,

it has been reported that the amount of intrinsic SEC's depends in part on the dislocation density.[22]

2. SEC's in AgCl doped with divalent cations

We first consider the SEC in AgCl doped with Pb^{2+}. Though the EPR signals of the SEC in AgCl:Pb^{2+} and the intrinsic SEC are similar, a comparison of the ENDOR spectra indicates that we are dealing with two distinctly different centers. First of all, the silver and chlorine ENDOR spectra displayed in Figs. 1 and 2 show that all transitions for the SEC in AgCl:Pb^{2+} occur closer to the Zeeman frequency than those of the intrinsic SEC. This indicates that the electron densities are smaller and therefore that the electron is more delocalized, as can also be seen from the radial dependences of Fig. 6. Second, there are some distinct differences in the ENDOR spectra of the two SEC's. In the ^{109}Ag spectrum of the SEC in AgCl:Pb^{2+} the transitions of the second and fourth silver neighboring shells are missing, whereas the transitions of the other shells occur at their simulated positions [see Fig. 7(a)]. In contrast, all chlorine shells can be traced back in the ^{35}Cl spectrum shown in Fig. 7(b), though the transitions of the first and the third chlorine neighboring shells are shifted toward higher and lower frequencies, respectively, compared to the simulation. The simulation is based on an unperturbed lattice which evidently does not represent the proper situation for these shells. Third, the observation of nuclear transitions of ^{207}Pb, shown in Fig. 3, proves that the SEC in AgCl:Pb^{2+} is related to lead. From the frequencies of these transitions we can derive from Eq. (3) that $(a/2)(^{207}\mathrm{Pb})=13.20\pm0.08$ MHz.

Based on the results of optical experiments, the Pb-related SEC was identified as an electron bound to a single Pb^{2+} ion.[4,23] In this model the divalent cation substitutes for silver and, though the surrounding ions might be slightly displaced from their lattice positions, they all should show up in the ENDOR spectra. The observation that the second silver shell (six ions at [200] positions) and the fourth silver shell (12 ions at [220] positions) are not present in the ^{109}Ag spectrum shown in Fig. 7(a), suggests that the ions of these shells are replaced either by vacancies or by other ions, most likely Pb^{2+}. This would indicate that the core of the Pb-related SEC studied by us consists of a Pb^{2+}-vacancy cluster rather than of a single Pb^{2+} ion. In order to attract an electron, the number of vacancies in such a cluster must be one less than the number of Pb^{2+} ions involved. Moreover, the vacancies and the divalent ions in the cluster must have a highly symmetrical distribution, since the analysis of the ENDOR data reveals that the binding core of the Pb-related SEC is centered on a cationic lattice position.

In Fig. 9, a possible structure for the binding core of the Pb-related SEC is sketched in which the silver ions of the second and fourth shells are replaced by vacancies and Pb^{2+} ions. A similar structure has been observed by x-ray studies of NaCl:Cd^{2+} crystals by Suzuki,[24] but no experimental proof of its existence in silver halides has been reported so far. It is, however, believed that its presence accounts for the observed behavior of the ionic conductivity of AgCl:Cd^{2+} at temperatures below 240 K.[25] In NaCl, Suzuki found that such a structure does not produce long-range disturbances in the NaCl lattice, but that the Cl^- ions inside this structure are slightly displaced toward the Cd^{2+} ions, whereas the Na^+ lattice ions retain their original lattice position. This would be in agreement with our observations. The ENDOR transitions of remote silver and chlorine shells do not split, and therefore indicate that no long-range disturbances are introduced in the lattice. The lines of the first, third, fifth, and higher silver shells can be simulated using an unperturbed lattice, indicating that the silver ions retain their original positions, whereas the shifts of the simulated transitions with respect to the observed lines of the first and third chlorine shells suggest that the ions in these shells are displaced [see Fig. 7(b)].

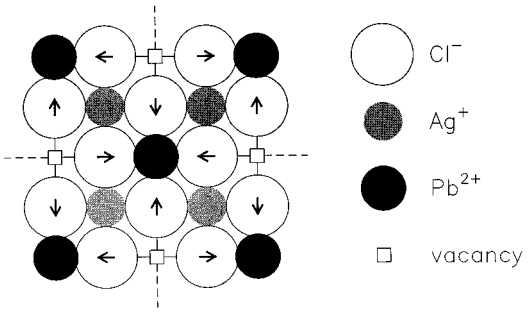

FIG. 9. [100] projection of a Pb^{2+}-vacancy cluster which possesses an excess Coulombic charge of $+1$, and is centered on a Ag^+-lattice position. The arrows indicate the displacements of the Cl^- ions.

The model of Fig. 9 contains five Pb^{2+} ions, of which four are equivalent and symmetrically placed around the fifth and central Pb^{2+}. For this situation, two ^{207}Pb ENDOR transitions are expected on each side of the nuclear Zeeman frequency, whereas only one transition is observed. Two possible explanations are that either the transition of the single central Pb^{2+} ion is just too weak for detection, or that an alternative model should be considered in which all Pb^{2+} ions in the cluster are equivalent. Calculations might be useful to check whether such small Pb^{2+}-vacancy clusters form a stable configuration.

We can make a rough estimate of the size of the cluster based on the observed EPR linewidth. In a similar way as described for the intrinsic SEC, we can calculate the full width at half maximum caused by the observed shf interactions of the silver and chlorine lattice ions. The deviation between this calculated value of 33.3×10^{-4} and the experimentally observed linewidth of $(34.6\pm0.5)\times10^{-4}$ (at 1.2 K) should reflect the contribution of the ^{207}Pb ions. Using Eq. (11) together with $(a/2)(^{207}\mathrm{Pb})=13.20\pm0.08$ MHz, we estimate that the number of incorporated Pb^{2+} ions is larger than one, but smaller than six. This points to rather small Pb^{2+}-vacancy clusters, in agreement with the observation that only two silver shells are replaced and that effects up to the fourth chlorine shell (containing six ions at [300] and 24 ions at [221]) are present.

Further support for the clusterlike segregation of Pb^{2+} ions and vacancies comes from the dependence of the EPR and ENDOR spectra upon heat treatment of the AgCl:Pb^{2+} crystal. Figure 4 shows the ^{109}Ag ENDOR spectra before, after 1 h, and after 22 h of annealing at 350 °C under Ar pressure followed by a rapid quench in water. The annealing procedure is expected to break up the clusters, whereas the

rapid quench freezes in the distribution obtained. Such a behavior is indeed reflected in Fig. 4. The spectrum of Fig. 4(a), characteristic of the clusterlike species, converts after 22 h of annealing to the spectrum of Fig. 4(c), which closely resembles the spectrum of the intrinsic SEC in the undoped crystal [see Fig. 1(b)]. The spectrum of Fig. 4(b) is seen to be a superposition of the two, and therefore illustrates that 1 h at 350 °C is too short to establish a complete conversion. The conversion may also be monitored through the ^{35}Cl ENDOR spectrum and, moreover, since the EPR linewidth of a SEC is mainly determined by the shf interaction, it is reflected by the measured linewidth of the SEC after each treatment. After storage of the sample at room temperature for several days, the cluster spectrum of Fig. 4(a) is retrieved, and apparently the process of breaking up the clusters at high temperatures and growing back at room temperature is reversible.

The result of the annealing treatment followed in Fig. 4 shows that the ENDOR spectrum characteristic of the intrinsic SEC finally becomes dominant. This appears to imply that, at a high annealing temperature of 350 °C, most of the Pb^{2+} ions liberated from the clusters are accompanied by charge-compensating (cationic) vacancies and, therefore, after having been frozen in by the quenching procedure and cooled down to 1.2 K, they are unable to act as traps for shallow electrons. Support for the appearance of such Pb^{2+}-vacancy pairs comes from the EPR study of Pb^{2+}-doped KCl, where these pairs are believed to exist after a similar heat treatment has been applied to the sample.[26] We do not believe that isolated Pb^{2+} ions can give rise to the intrinsic spectrum, as recorded in undoped AgCl crystals that have been stored at room temperature for months, because the observed SE intensity in the undoped crystal would require a concentration of the Pb^{2+} ions at which clusters should already have been formed. Moreover, with its closed-valence-shell structure, the incorporation of a single Pb^{2+} ion is not expected to introduce a defect symmetry lower than the cubic symmetry of the lattice. As discussed in Sec. V B 1, the splitting of some of the lines in the intrinsic ENDOR spectrum indicates that the defect symmetry is more likely D_{2h}.

In the case of a SEC formed in AgCl:Cd^{2+}, the results are less clear. The ENDOR transitions of silver and chlorine are shifted further away from the corresponding Zeeman frequencies than those of the Pb-related and intrinsic SEC's (see Figs. 1 and 2). This indicates that the SEC's in AgCl:Cd^{2+} are more localized, as shown by the radial dependences of Fig. 6. Since the pattern of the chlorine ENDOR spectrum closely resembles that of the Pb-related SEC, and because the transitions of the second and fourth silver shells are again missing, the SEC's in AgCl:Cd^{2+} most likely also consist of electrons trapped at Cd^{2+}-vacancy clusters instead of being trapped at single Cd^{2+} ions substituting for silver. The only marked difference is that, in contrast to AgCl:Pb^{2+}, the ENDOR transition of the sixth silver shell, containing eight nuclei at [222] lattice positions, appears to be missing or perhaps shifted to a slightly higher frequency [see Fig. 1(c)]. This suggests that the ions of the sixth silver shell are partially replaced, and therefore the Cd^{2+}-vacancy cluster should be larger than the Pb^{2+}-vacancy cluster discussed above, i.e., it contains more than six Cd^{2+} ions. As the second, fourth, and sixth silver shells contain in total 26 lattice positions, and since the sixth shell is only partially replaced, we estimate an upper limit of 13 Cd^{2+} ions, which have to be accompanied by 12 silver vacancies to obtain the total Coulombic charge of $+1$.

Unfortunately, no ENDOR transitions of ^{111}Cd ($I=\frac{1}{2}$, 12.8%) were observed in the region up to the ^{111}Cd Zeeman frequency around 33 MHz in a specially prepared ^{111}Cd-enriched crystal. Therefore no direct information concerning the core of the Cd-doped SEC could be obtained. Because the silver and chlorine ENDOR lines were considerably broadened as compared to the normal sample, it might be that the ^{111}Cd transitions are smeared out as well, and consequently not observable. This broadening of the ENDOR lines and the observation that the EPR linewidth narrowed from $(56\pm1)\times10^{-4}$ T for the normal sample to $(53\pm1)\times10^{-4}$ T for the ^{111}Cd-enriched crystal suggests that the doping level in the latter one was so high that impurity bands were created. An alternative explanation might be that the low-frequency transitions of the Cd isotopes are hidden under the silver or chlorine ENDOR spectra.

Table II shows that the energy difference E_{1s-2p} calculated for the Cd^{2+}-related SEC by both the simple effective-mass approach and the quantum-defect method is in line with the trend observed for the various SEC's in AgCl, but that the absolute value does not correspond with the observed value reported by Sakuragi and Kanzaki.[4] This might be related to the small bromine contamination of the AgCl:Cd^{2+} crystal studied by us, shown by the appearance of the bromine-related STH in the EPR spectrum. Since the electron g factor for mixed $AgCl_{1-x}Br_x$ crystals is known to exhibit a linear relationship with concentration,[2] we estimate the contamination level to be at most 0.65%, based on the small shift of the g value from 1.878 (in the case of the intrinsic and Pb-related SEC's) to 1.876 (for the Cd-related SEC). In principle, the presence of bromine will affect the values of the static dielectric constant and the polaron mass involved in the energy calculations. However, since the concentration is very small, we believe this effect to be of minor importance. It seems more likely that the discrepancy in the observed and calculated value of E_{1s-2p} indicates that the Cd-related SEC studied by Sakuragi and Kanzaki is not identical to the one studied by us. Since the ENDOR spectra suggest that the central cluster in the Cd-related SEC is larger than in the Pb-related SEC (for which we obtain a good agreement between the optical and ENDOR results) the Cd-related SEC studied by us probably contains more Cd^{2+} ions and silver vacancies.

In a AgBr crystal doped with 100 mppm Pb^{2+}, we recorded a SEC signal with a linewidth of $(124\pm5)\times10^{-4}$ T at a g value slightly higher ($\sim$0.1%) than that of the SEC in undoped AgBr. Since the linewidth is considerably smaller than the value of $(160\pm5)\times10^{-4}$ T for the intrinsic SEC in AgBr, and because we have shown that the linewidth of a SEC is mainly determined by the shf interaction, we may conclude that the Pb-related SEC is more delocalized than the intrinsic SEC, in agreement with the situation in AgCl. Unfortunately, in the AgBr:Pb^{2+} sample the spin-lattice relaxation of the SEC turned out to be too fast to perform the pulsed ENDOR experiment, and moreover the coupling of the cavity to the microwave bridge appeared to be poor.

TABLE IV. Columns 2, 3, and 4 contain the total silver, chlorine, and bromine shf interactions estimated from the ENDOR spectra of the various SEC's in AgCl and AgBr. In the last three columns the isotropic hf interactions for unit spin density in atomic orbitals (specified by their quantum numbers n and l) are listed, derived from the values calculated by Morton and Preston (Ref. 28). As explained in Sec. V C, the values in the sixth column represent upper limits.

AgCl	Cd^{2+}	undoped	Pb^{2+}	$^{109}Ag(5s)$	$^{35}Cl(4s)$	$^{35}Cl(3s)$
$a_{total}(^{109}Ag)$ (MHz)	1990	2220	2040	1974		
$a_{total}(^{35}Cl)$ (MHz)	1830	2000	1860		<447	5368
AgBr		undoped		$^{109}Ag(5s)$	$^{81}Br(5s)$	$^{81}Br(4s)$
$a_{total}(^{109}Ag)$ (MHz)		2170		1565		
$a_{total}(^{81}Br)$ (MHz)		12060			<2103	25707

These two observations indicate that the 100-mppm doping level of Pb^{2+} is too high, and gives rise to conduction resulting from the formation of an impurity band. In AgCl the delocalization of trapped electrons is less than in AgBr, and at a concentration of 100 mppm impurity bands are apparently not yet formed.

C. Character of the lowest conduction-band state

Various methods have been applied to compute the electronic band structures of silver halides.[17] The band structures of AgCl and AgBr are qualitatively similar, and the lowest conduction band is believed to be simple and s like with a minimum at the Γ point. According to Fowler, the lowest state of the conduction band even appears to be largely Ag s like.[27] Since EMT implies that a shallowly trapped electron strongly resembles a conduction electron [see, for instance Eq. (5)], the study of SEC's in AgCl and AgBr will yield information concerning the nature of the conduction bands. EPR reveals that the SEC's possess g values of $g\sim1.88$ in AgCl, and $g\sim1.49$ in AgBr, which deviate considerably from $g=2.0023$.[2] This implies that spin-orbit coupling is involved, and indicates that the conduction band is not purely s like. The fact that in the present study the ENDOR spectra of both the silver and halide ions are observed, shows that the shallowly trapped electron besides interacting with Ag^+ also interacts with the Cl^- and Br^- lattice ions. This observation demonstrates that not only Ag s-like but also halide s-like characters are involved in the lowest state of the conduction band. In this section we will try to obtain a more quantitative description.

In columns 2, 3, and 4 of Table IV, we list the total silver and halide shf interactions which have been estimated from the ENDOR spectra. These estimates are based on the envelope functions (6) derived for the various SEC's and the proportionality constants of Table I. From the ENDOR study of the self-trapped exciton in AgCl,[8] the spin density of a shallowly trapped electron was concluded to be positive on both the silver and chlorine lattice ions. In an atomistic picture, the positive spin density on Ag^+ can be understood if one assumes the wave function of the shallow electron to be built up predominantly of the vacant $5s$ orbitals of the Ag^+ lattice ions. The isotropic hf interaction for unit spin density on the atomic $5s$ orbital of ^{107}Ag has been calculated by Morton and Preston for $g_e=2.0023$.[28] We included the value for ^{109}Ag in Table IV after correcting for the proper g-values of 1.878 and 1.489 of the SEC's in AgCl and AgBr, respectively. Though these calculated values are slightly smaller than the total shf interactions estimated from the ENDOR spectra, the order of magnitude is similar for both AgCl and AgBr. Apparently, the observed total silver shf in both materials can be accounted for when the shallowly trapped electron is mainly localized in $Ag(5s)$ orbitals. The observed spin density on chlorine might, in principle, result from the overlap of the neighboring $Ag(5s)$ orbitals with the chlorine nucleus. We shall neglect such overlap, since it cannot account for the large chlorine shf interactions observed. The positive spin density on chlorine can then be explained if the shallow electron occupies the vacant $4s$ orbital of the Cl^- ion. Though the isotropic hf interaction for unit spin density on the $Cl^-(4s)$ orbital is unknown, we can make an estimate from the value for potassium calculated by Morton and Preston.[28] Owing to the higher nuclear charge of potassium ($Z=19$) compared to chlorine ($Z=17$), the $4s$ orbital will be more strongly localized at the potassium nucleus compared to the chlorine nucleus and the estimated value for chlorine will consequently represent an upper limit. We included this upper limit for $^{35}Cl(4s)$ in column 6 of Table IV, and it is clear that the total chlorine shf interaction derived from the ENDOR spectra is much larger. This suggests that some character of lower-lying chlorine s states is involved which induces much larger hf interactions, as illustrated by the value for unit spin density on $^{35}Cl(3s)$ listed in column 7 of Table IV.[28]

Although, for bromine, the sign of the shf coupling is not known, a similar picture can be obtained from the total shf interaction of bromine derived from the ENDOR of the SEC in undoped AgBr. The upper estimate for unit spin density on the $5s$ orbital of Br^-, based on the value calculated for atomic rubidium,[28] is much smaller than the value derived from the experiment suggesting the participation of lower-lying s orbitals of Br^- (see Table IV). Therefore, as the sum of the total shf interactions of the silver and halide ions is much larger than the values estimated for unit spin density on atomic orbitals, a description of the shallowly trapped electron in terms of a simple one-electron wave function consisting solely of $Ag^+(5s)$ and $Cl^-(4s)$ orbitals in the case of AgCl, and of $Ag^+(5s)$ and $Br^-(5s)$ orbitals in the case of AgBr, seems inappropriate. One needs at least to use a many-electron approach in which the interaction between the shallow electron and the core electrons of the halide lattice ions is included.

A possible many-electron description is that (in zeroth order) the shallow electron occupies mainly $Ag(5s)$ orbitals, whereas a (first-order) correction follows from the polarization of the halide s core electrons induced by the electron density on the neighboring silver ions. In this description, the order of magnitude of the observed total shf interactions of silver, chlorine, and bromine can be understood based on the atomic $Ag(5s)$, $Cl(3s)$, and $Br(4s)$ orbitals. This approach is reasonable when the atomic orbitals are not strongly modi-

fied by the effects of the crystal potential and covalency.[11] However, the inspection (given below) of the proportionality constants of Ag, Cl, and Br listed in Table I, illustrates that these effects cannot be neglected for the silver halides, and therefore that such a simplistic many-electron description is not justified.

As mentioned in Sec. IV, the proportionality constants in ionic crystals can be obtained by orthogonalization of the envelope function of the shallow electron to the wave functions of the core electrons of the lattice ions. In Table I we included the values obtained by the Schmidt orthogonalization procedure using the envelope functions derived from experiment together with the functions given by Clementi and Roetti for the core electrons of free Ag^+, Cl^-, and Br^- ions.[29] For AgCl the calculated proportionality constant of Ag is a factor 3.7 smaller than the experimentally derived value, whereas for Cl this factor equals about 1.9. For AgBr, the deviation of the calculated value with respect to the observed one is again larger for Ag than for Br, a factor of 5.5 and 3.0, respectively. An alternative method which relies on the EMT description of the wave function of a shallow donor in a semiconductor confirms the values obtained for Ag and Cl. In EMT the proportionality constant for nucleus α equals $|u(\mathbf{k}_0,\alpha)|^2$ with $u(\mathbf{k}_0,\mathbf{r})$, the lowest Bloch function of the conduction band. If we follow the method introduced by Krumhansl for KCl,[30] in which the value of $u(\mathbf{k}_0,\alpha)$ at the silver nucleus is given by the ratio of the atomic Ag($5s$) orbital at the nucleus to its value at the outer maximum, we can calculate the value for $|u(\mathbf{k}_0,\mathrm{Ag})|^2$ using the $5s$ orbital given by Clementi and Roetti.[29] Gourary and Adrian[10] argue that this method is reasonable to account for the rapid oscillations of $u(\mathbf{k}_0,\mathbf{r})$ in the immediate vicinity of the nucleus. Dexter[31] calculated in a similar method the proportionality constant of chlorine based on the $4s$ function of Cl^- determined by Tibbs in case of NaCl.[32] The values of $|u(\mathbf{k}_0,\alpha)|^2$ for silver and chlorine are included in Table I, and these values agree with the trend and the order of magnitude of the proportionality constants calculated by the method valid for ionic crystals.

The deviation between the calculated and observed proportionality constants of Table I reflects the fact that the free atomic and ionic orbitals, on which the calculations are based, apparently differ considerably from the orbitals of the ions in the crystal. Consequently, the interpretation of the observed total silver and halide shf interactions, listed in Table IV, in terms of the hf interactions for unit spin density on free atoms, as given by Morton and Preston,[28] seems very unreliable. Though the results of Table IV reveal qualitatively that the wave function of the SEC's in AgCl and AgBr is not mainly Ag s like, but that a substantial amount of Cl s character is involved as well, it is not possible to obtain a more quantitative description. Any serious attempt to give such a detailed description of the wave function of a SEC in silver halides, and thus of the lowest state of the conduction band, should be a many-electron approach leading to improved ionic orbitals.

It may be noted that, since the silver proportionality constants deviate more strongly than those of the halide ions, it appears that the Ag^+ orbitals are more strongly modified in the crystal than those of Cl^- and Br^-. The silver ion is indeed believed to be deformable in the AgCl lattice, since modeling studies of the silver mobility in AgCl indicate that the low activation energy can be attributed to this property.[33] For chlorine the observed proportionality constants deviate only about a factor of 2 from those calculated, which suggests that the orbitals of the free chlorine ion are not that strongly altered in the crystal. From an ENDOR study of F centers in NaCl, a proportionality constant of 967 has been derived for chlorine.[34] The close correspondence between this value and the average value of 1301 derived by us indicates that the core orbitals of chlorine are indeed not so strongly dependent on the host lattices NaCl or AgCl. For Br^-, a value of 1960 has been derived in NaBr.[34] The larger deviation with the value of 4220 derived for AgBr suggests that the bromine orbitals are more dependent on the host lattice.

VI. CONCLUSIONS

The results of the ENDOR study presented in this paper reveal information about the microscopic structure of several Coulombic centers, which act as shallow traps for electrons. For all SEC's studied by us, the Coulombic core is centered on a Ag^+-lattice position. We propose that, in undoped AgCl and AgBr, the core is formed by a split-interstitial silver pair, though it is not really clear in which direction such a pair should point. This model for the intrinsic (shallow) electron center in silver halides can be viewed as the antipode of the intrinsic electron center formed in alkali halides, which consists of an electron deeply trapped at an anion vacancy (the F center).[35] In AgCl crystals doped with the divalent, closed-shell ions Pb^{2+} and Cd^{2+}, small cation-vacancy clusters are formed which can capture electrons as well. The results of a heat treatment applied to the AgCl:Pb^{2+} crystal suggest that these clusters break up at high temperatures, thereby forming isolated Pb^{2+} ions accompanied by charge-compensating cation vacancies. Such pairs are believed to be formed in Pb^{2+}-doped KCl as well.[26]

The spin-density distribution derived from the silver and halide ENDOR spectra for the ground state of the various SEC's, largely resembles a hydrogenlike $1s$ behavior. It appears that a simple hydrogen model can successfully be applied for the estimation of the optical transition energies of the intrinsic and Pb-related SEC in AgCl and of the intrinsic SEC in AgBr. The more realistic quantum-defect method confirms that the short-range potential, introduced by the Coulombic trap, is repulsive, and shows that the polaron mass and the static dielectric constant are appropriate for the description of the $1s$-like ground state.

Theoretical work is needed for a detailed description of the wave function of the SEC's, which strongly resembles the Bloch function of the lowest state of the conduction band. The observed silver and halide shf interactions cannot be accounted for in the usual one-electron or the discussed (simplistic) many-electron approaches, where the hf interactions of free atoms are used as a reference. Owing to the covalent character of the highly ionic silver halide lattice, the ionic orbitals in the crystal are strongly modified, which makes these approaches very unreliable.

ACKNOWLEDGMENTS

This work forms part of the research program of the ''Stichting voor Fundamenteel Onderzoek der Materie''

(FOM) with financial support from the ''Nederlandse Organisatie voor Wetenschappelijk Onderzoek'' (NWO). Further support was obtained from the HCM program of the Commission of the European Community under Contract Nos. ERBCHRXCT93028 and ERBCIPDCT940612. The authors wish to thank Dr. R. S. Eachus, Dr. A. J. Zakrzewski, Professor J. H. van der Waals, and Professor A. M. Stoneham for very stimulating discussions.

[1] J. F. Hamilton, in *The Theory of the Photographic Process*, edited by T. H. James (Macmillan, New York, 1977).
[2] A. P. Marchetti and R. S. Eachus, Adv. Photochem. **17**, 145 (1992).
[3] R. C. Brandt and F. C. Brown, Phys. Rev. **181**, 1241 (1969).
[4] S. Sakuragi and H. Kanzaki, Phys. Rev. Lett. **38**, 1302 (1977).
[5] M. T. Bennebroek *et al.*, Phys. Rev. Lett. **74**, 442 (1995).
[6] W. B. Mims, in *Electron Paramagnetic Resonance*, edited by S. Geschwind (Plenum, New York, 1972).
[7] J. A. J. M. Disselhorst *et al.*, J. Magn. Reson. A **115**, 183 (1995).
[8] M. T. Bennebroek *et al.*, Phys. Rev. B **53**, 15 607 (1996).
[9] B. S. Gourary and F. J. Adrian, Phys. Rev. **105**, 1180 (1957).
[10] B. S. Gourary and F. J. Adrian, in *Solid State Physics*, edited by F. Seitz and D. Turnbull (Academic, New York, 1960), Vol. 10, p. 127.
[11] A. M. Stoneham, *Theory of Defects in Solids* (Clarendon, Oxford, 1985).
[12] K. W. Böer, *Survey of Semiconductor Physics* (Van Nostrand Reinhold, New York, 1990).
[13] M. Matsuura, J. Phys. Soc. Jpn. **53**, 284 (1984).
[14] K. K. Bajaj and T. D. Clark, Phys. Status Solidi B **52**, 195 (1972).
[15] M. Ueta *et al.*, in *Excitonic Processes in Solids*, Springer Series in Solid State Sciences Vol. 60 (Springer-Verlag, Berlin, 1986).
[16] J. Adamowski, Phys. Rev. B **32**, 2588 (1985).
[17] W. von der Osten, in *Semiconductors, Physics of II-VI and I-VII Compounds, Semimagnetic Semiconductors*, edited by K.-H. Hellwege and O. Madelung, Landolt-Börnstein, New Series, Group III, Vol. 17, Pt. b (Springer, Berlin, 1982).
[18] R. A. Zhitnikov, P. G. Baranov, and N. I. Melnikov, Phys. Status Solidi B **59**, k111 (1973).
[19] R. C. Baetzold and R. S. Eachus, J. Phys. C **7**, 3991 (1995).
[20] S. Seidel and H. C. Wolf, in *Physics of Color Centers*, edited by W. B. Fowler (Academic, New York, 1968).
[21] K. S. Song and R. T. Williams, *Self-Trapped Excitons* (Springer-Verlag, Berlin, 1993).
[22] R. S. Eachus *et al.*, Phys. Status Solidi B **152**, 583 (1989).
[23] H. Kanzaki, Photog. Sci. Eng. **24**, 219 (1980).
[24] K. Suzuki, J. Phys. Soc. Jpn. **16**, 67 (1961).
[25] K. Zierold, M. Wentz, and F. Granzer, J. Phys. **34**, 415 (1973).
[26] P. G. Baranov and V. A. Khramtsov, Phys. Status Solidi B **101**, 153 (1980).
[27] W. B. Fowler, Phys. Status Solidi B **52**, 591 (1972).
[28] J. R. Morton and K. F. Preston, J. Magn. Res. **30**, 577 (1978).
[29] E. Clementi and C. Roetti, At. Data Nucl. Data Tables **14**, 177 (1974).
[30] J. A. Krumhansl, Phys. Rev. **93**, 245 (1954).
[31] D. L. Dexter, Phys. Rev. **93**, 244 (1954).
[32] S. R. Tibbs, Trans. Faraday Soc. **35**, 1471 (1939).
[33] P. W. M. Jacobs, J. Corish, and C. R. A. Catlow, J. Phys. C **13**, 1977 (1980).
[34] W. C. Holton and H. Blum, Phys. Rev. **125**, 89 (1962).
[35] W. Hayes and A. M. Stoneham, *Defects and Defect Processes in Nonmetallic Solids* (Wiley, New York, 1985).
[36] J. Corish and P. B. Fitzsimons, Philos. Mag. A **56**, 1 (1987).
[37] C. Gemperle and A. Schweiger, Chem. Rev. **91**, 1481 (1991).